ACS Partner Journal
PRECISION CHEMISTRY

pubs.acs.org/PrecisionChem
Article

Synthesis of Alternatively-Twisted Nanographenes by Semi-Deprotection-Induced Cyclization

Zhenxun Xu, Suriguga Meng, Zhiyu Zhang, Shuqin Han,* Fenghua Bai,* Yanping Dong, Yoshifumi Hashikawa,* and Chaolumen*

Cite This: *Precis. Chem.* 2025, 3, 289−294
Read Online

ABSTRACT: Twisted nanographenes (NGs) are currently attracting a lot of attention owing to their geometrical and electronic structures that differ substantively from conventional planar and nonplanar NGs, while the strategic synthesis of twisted NGs is still a topic of interest because the products are often interconvertible among unidirectionally, alternatively, or randomly twisted geometries and otherwise obtained as a mixture of them. Herein, we report the conformationally specific synthesis of twisted NGs where the geometry was reinforced by introducing 1,4-dioxane rings at a K-region of a central pyrene core that bears a large contortion. The 1,4-dioxane rings were generated by semi-deprotection, of tetraoxa[4.4.4]propellanes in precursor molecules, which were confirmed to be engaged in forming C−C bonds via a Friedel−Crafts type mechanism. The large contortion within the pyrene core causes a narrowed HOMO−LUMO gap on account of unusual p_z-lobe overlap between $+z$ and $-z$ sides, giving rise to red emission with a high quantum yield of 94% as well as stable redox processes of $2e^-$ uptake/release.

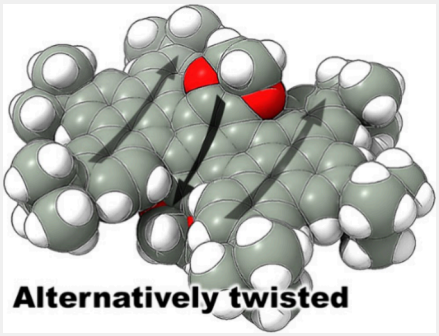

KEYWORDS: *Conformation, Nanographene, Red Emission, Semi-Deprotection, Twist*

INTRODUCTION

The twist operation is often employed to enhance the chemical stability of polyacenes against their dimerization and/or spontaneous air oxidation,[1−5] where the twist geometry does not significantly change electronic structures compared to those of pristine polyacenes,[6] although there are a few exceptions. For instance, 1,8-diadamantylnaphthalene bearing a twist angle of 17.0° showed a clear red shift in its absorption band relative to parent naphthalene (323 from 264 nm), as reported by Yamaguchi and co-workers in 2013. This is primarily due to elevated HOMO level caused by σ-conjugation with substituents after twisting.[7,8] In 2018, the group led by Gidron also reported a bathochromic shift (427 from 407 nm, twist angle of 30.0°) in twisted anthracenes diagonally tethered by an *n*-alkyl bridge.[9] This is caused by a lowered LUMO level from twisting, which also contributes to a slight increase in the absorption coefficient owing to decreased symmetry rendering the transition vibronically allowed.

Alongside twisted polyacenes, the synthesis of simple twisted PAHs (polycyclic aromatic hydrocarbons) has received growing attention[10,11] for developing CPL (circularly polarized light) emitters.[12,13] The twist-induction is usually performed by introducing bully substituents at the bay area[14−18] or by propagation of chiral strain from the ends.[19,20] However, once the π-core changes to nanographenes (NGs), the study of the twisting effect becomes particularly difficult due to their interconvertible conformations among unidirectionally, alternatively, or randomly twisted conformations and even wavy structure (Figure 1).[21−23] Therefore, the synthesis of conformationally pure twisted NGs is still a formidable challenge,[24−27] and rational logic for geometrical reinforcement is highly

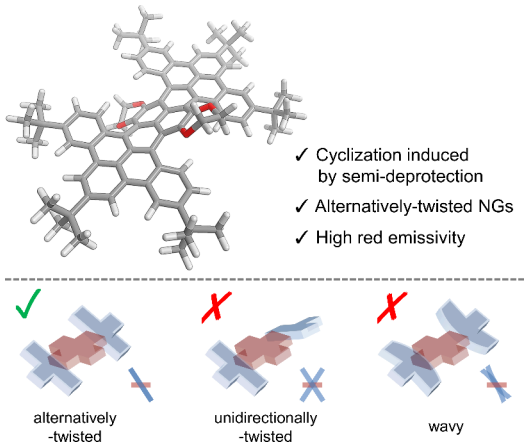

Figure 1. An alternatively twisted nanographene.

Received: January 2, 2025
Revised: March 5, 2025
Accepted: March 6, 2025
Published: March 13, 2025

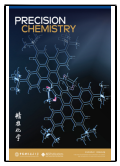

https://doi.org/10.1021/prechem.5c00001
Precis. Chem. 2025, 3, 289−294

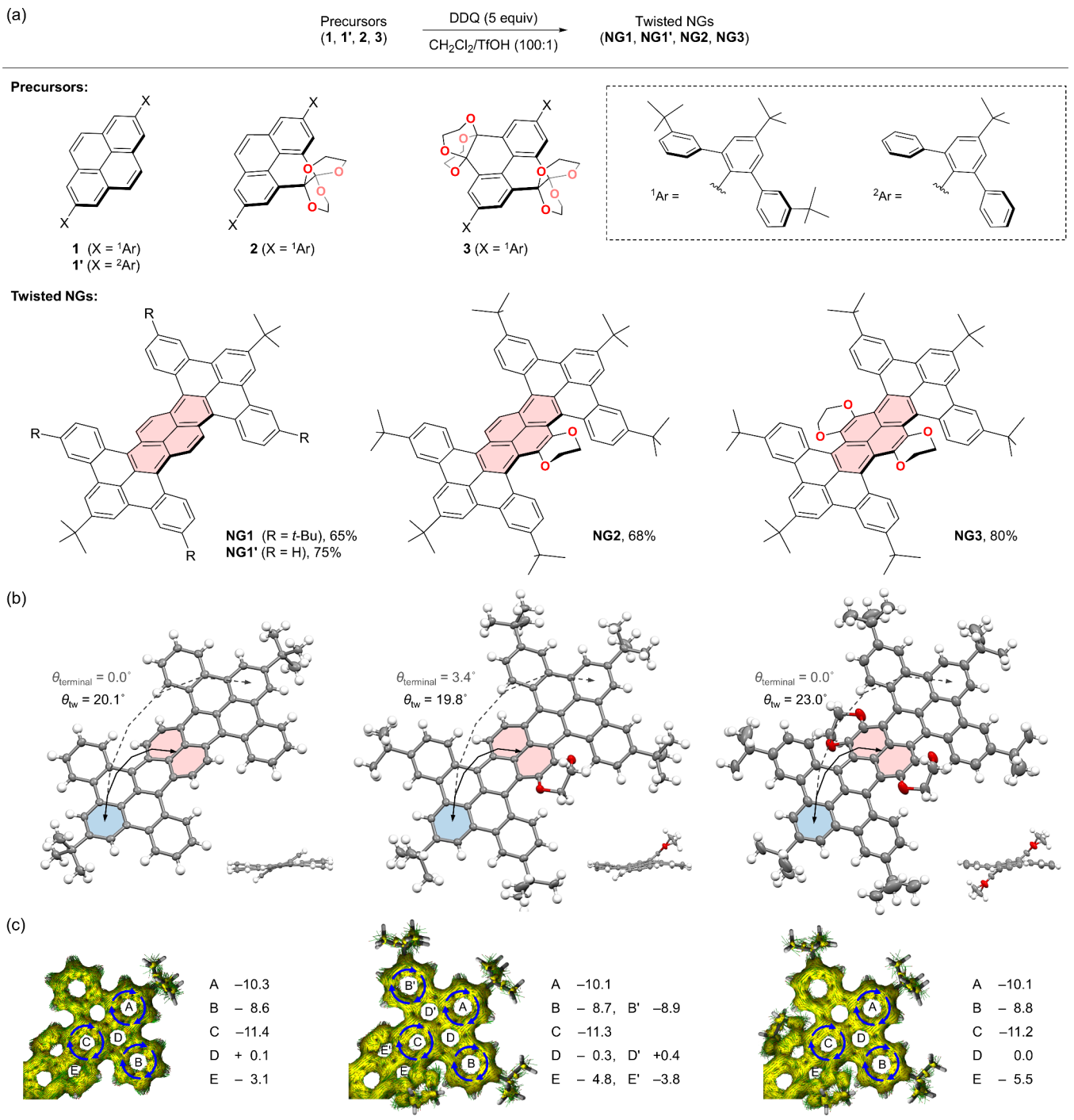

Figure 2. (a) Synthesis of alternatively twisted NGs (DDQ, 2,3-dichloro-5,6-dicyano-*p*-benzoquinone; Tf, CF_3SO_2), (b) crystal structures showing thermal ellipsoids at 50% probability (solvent molecules and *t*-Bu groups are omitted in side views for clarity), and (c) ACID (anisotropy of current-induced density) plots with NICS(0) (nucleus-independent chemical shifts, units in ppm) values in rings A–E (HF/6–31+G(d,p)//B3LYP-D3/6–31G(d)).

demanded. Very recently, we reported a twisted NG wherein 2-fold unidirectionally twisted skeletons are orthogonally arranged around a contorted pyrene core, which behaves as an origin of both chirality and high emissivity.[28] At the nearly same time, Pun and co-workers also reported the related structures.[29] In this Article, we report the synthesis of alternatively twisted NGs with a pyrene core used as a fluorophore (Figure 1), wherein the introduction of fused 1,4-dioxane rings at the K-region on the pyrene core allows the NGs to adopt an alternatively twisted geometry as the sole conformation. This geometrical reinforcement was unprecedentedly achieved by semi-deprotection of tetraoxa[4.4.4]propellane placed on the pyrene core, importantly, the semi-deprotection was disclosed to be engaged in NG-generation (C–C bond formation) through Friedel–Crafts-type processes.

https://doi.org/10.1021/prechem.5c00001
Precis. Chem. 2025, 3, 289–294

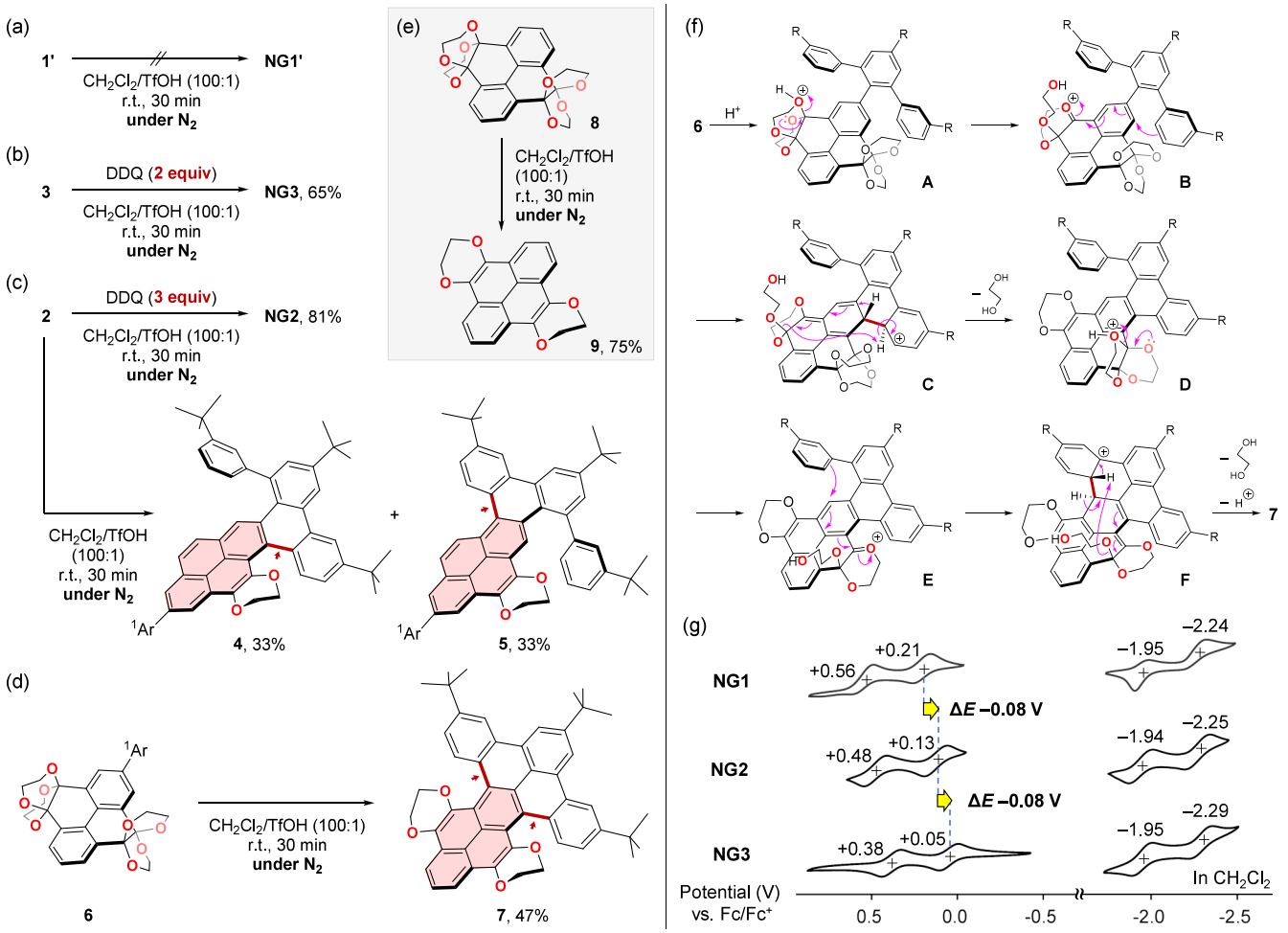

Figure 3. (a–e) Control experiments using **1′**, **2**, **3**, **6**, and **8** in the absence of DDQ or with reduced stoichiometry of DDQ. (f) Plausible mechanism. (g) Cyclic voltammograms of **NG1**, **NG2**, and **NG3** (1 mM in CH_2Cl_2, 0.1 M *n*-$Bu_4N{\cdot}PF_6$, 100 mV/s).

RESULTS AND DISCUSSION

Synthesis

The Scholl cyclization of arylated pyrenes **1**–**3**, which were prepared from the corresponding aryl bromides and borylated pyrene backbones via Suzuki–Miyaura coupling, was carried out to obtain **NG1**–**NG3** in 65–80% yields (Figure 2a). During the reaction, the tetraoxa[4.4.4]propellane moieties in **2** and **3** were semi-deprotected to regenerate the pyrene skeleton with fused 1,4-dioxane ring(s) at the K-region. The structures of **NG1**–**NG3** were determined crystallographically, revealing that all three NGs adopt an alternatively twisted geometry in the solid state (Figure 2b). The repeating twist angles (θ_{tw}) were measured as **NG1′** (20.1°) ≈ **NG2** (19.8°) < **NG3** (23.0°), while end-to-end angles ($\theta_{terminal}$) are almost close to 0°. According to theoretical calculations, the introduction of the 1,4-dioxane ring(s) to **NG1** does not cause significant alteration of the aromaticity with the retention of the original benzenoid characters (Figure 2c).

Mechanism

During the course of this study, we were aware of a curious fact that **NG2** and **NG3** could be produced as usual even under the poor stoichiometry of DDQ (Figures 3b, c) while **NG1** does offer DDQ (Figure 3a). Importantly, even in the absence of DDQ, **2** underwent a ring-fusion to furnish **4** and **5**, both in 33% yields, where one of the four requested bonds was generated simultaneously with the semi-deprotection of the tetraoxa[4.4.4]propellane moiety (Figure 3c). This indicates that semi-deprotection compensates a stoichiometric C–C bond formation. This would be a cause of the efficient generation of **NG2** and **NG3** with the poor stoichiometry of DDQ (Figures 3b, c). If this is the case, the synthesis of NGs would be probable with a designed precursor containing tetraoxa[4.4.4]propellane moieties, even without offering any oxidant such as DDQ and air. To confirm this hypothesis, **6** was subjected to acidic media in the absence of oxidant under inert conditions (Figure 3d). As the results, the corresponding twisted NG (**7**) was obtained in 47% yield via cyclization induced by 2-fold semi-deprotection. It should be noted that **8** could also undergo semi-deprotection to give **9** via a different pathway where it needs to borrow two electrons, presumably from released ethylene glycol[30–33] or via release of glycolglycolaldehyde (Figure S58).

Based on the aforementioned observation, we illustrated the plausible mechanism in Figure 3f. The reaction commences with protonation at the tetraoxa[4.4.4]propellane moiety (**A**), which induces a C–O cleavage to generates **B**. Then, intramolecular Friedel–Crafts-type cyclization takes place to give **C**. The release of the first ethylene glycol furnishes **D**, which further undergoes the second cyclization (**E** to **F**) and loss of ethylene glycol to yield **7**.

https://doi.org/10.1021/prechem.5c00001
Precis. Chem. 2025, 3, 289–294

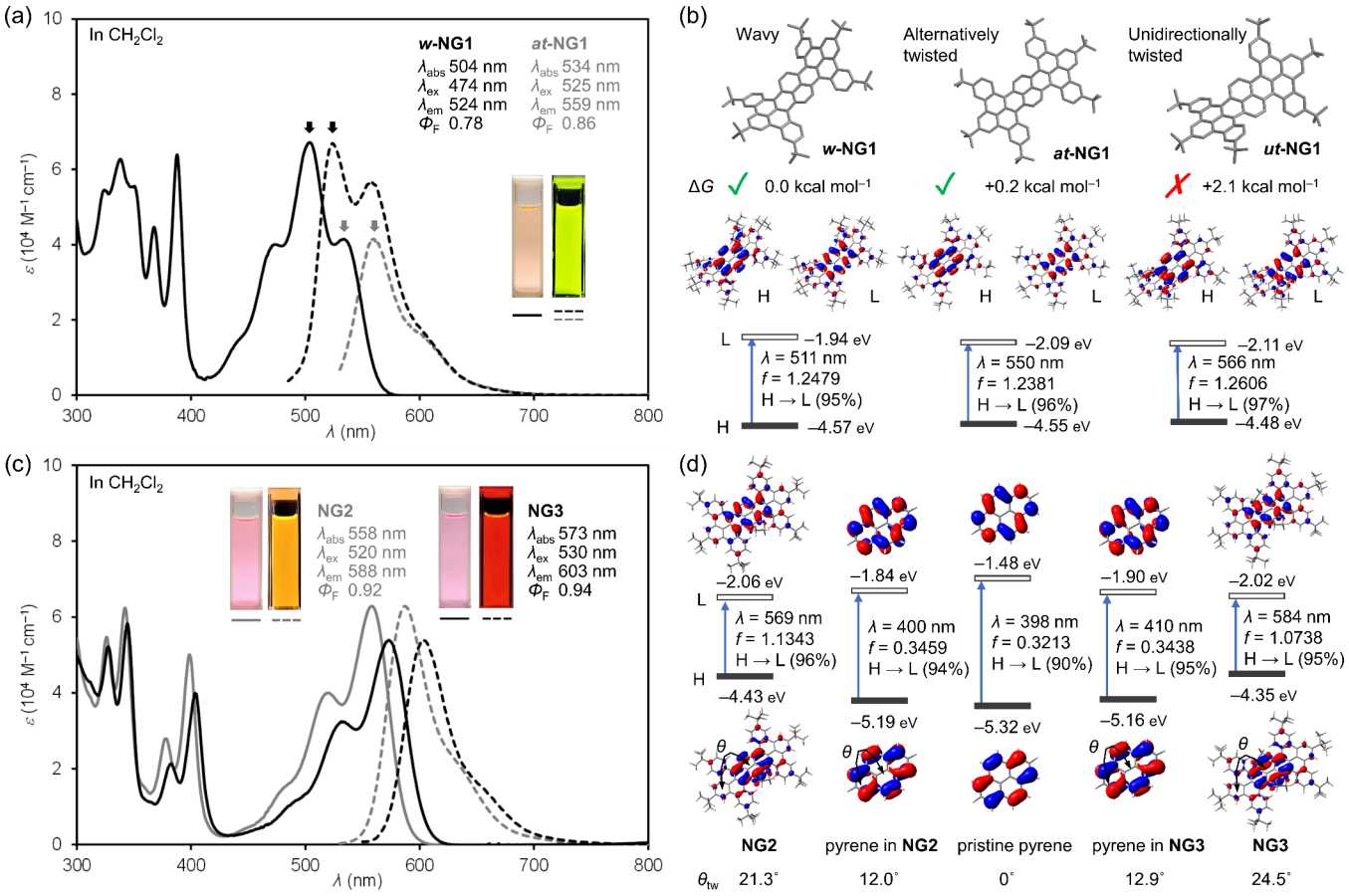

Figure 4. (a, c) Absorption (5.0 μM) and fluorescence (1.2 μM) spectra of **NG1**–**3**. (b, d) MO energy levels and optical transitions of **NG1** with possible conformations as well as **NG2** and **NG3** with their segmental pyrene structures. The relative Gibbs energies were computed at 298 K, and transition energies were scaled by 0.88 (TD-CAM-B3LYP-D3/6–31G(d)//B3LYP-D3/6–31G(d)).

Electrochemistry

Cyclic voltammograms revealed high redox stability upon $2e^-$ release/uptake for all NGs examined (Figure 3g). Though the reduction potentials are almost comparable to each other, the first oxidation waves showed a gradual cathodic shift upon increasing a count of electron-donating 1,4-dioxane ring(s) in the order of **NG1** (E_{ox}^1 + 0.21 V) > **NG2** (+0.13 V) > **NG3** (+0.05 V).

Photophysical Properties

NG1 exhibited two major absorption bands at 504 and 534 nm, both of which were identical to fluorescence spectra centered at 524 and 559 nm, respectively (Figure 4a). The excitation spectra with an λ_{ex} of 559 nm clearly suggested the presence of two components for **NG1** (Figure S57). This is supported by theoretical calculations telling that the wavy conformation (*w*-**NG1**) is the most thermodynamically stable form in the gas phase, while the second is alternatively twisted geometry (*at*-**NG1**) (Figure 4b). Since the unidirectionally twisted geometry (*ut*-**NG1**) is less stable compared with the other two, **NG1** is considered to fluctuate between the two distinctive conformations in solution within the measured time range, though we could not discriminate the two conformations by NMR study, probably because of the conformational change occurring at the NMR time scale even at 238 K (Figure S19). From transition energies computed, the absorption/emission bands at the longer wavelength were characterized to be *at*-**NG1** with another being *w*-**NG1**.

Different from those of **NG1**, the spectral feature of **NG2** and **NG3** is readily understandable. The introduction of the 1,4-dioxane ring(s) caused a bathochromic shift in the lowest-energy transition in the order of **NG1** (λ_{abs} 534 nm, λ_{em} 559 nm) < **NG2** (558, 588 nm) < **NG3** (573, 603 nm) (Figure 4c), reflecting the narrower HOMO–LUMO gap triggered by the elevated HOMO level (Figure 4d). Thus, the emission color changes from greenish yellow (**NG1**) to orange (**NG2**) and then red (**NG3**) while maintaining high quantum efficiency Φ_F of 78–94%. The absence of multiple absorption/emission bands for **NG2** and **NG3** simply suggests the sole conformation as is also supported by computations suggesting that the alternatively twisted geometry is the most stable form and the second stable geometry, that is, a wavy or unidirectionally twisted form, is more labile by ΔG > +4 kcal/mol. This geometrical reinforcement is also evident from the smaller Stokes shifts of 41 eV for **NG2** and **NG3** compared with 62 eV for *w*-**NG1** and 50 eV for *at*-**NG1**. The primary contributor to enhance the structural rigidity and/or stabilization of the alternatively twisted geometry is the 1,4-dioxane ring(s) fused at the K-region.

To verify the effect of contortion occurring at the central pyrene core, we examined the electronic structures of **NG2** and **NG3**. The optimized geometries have repeating twist angles of 21.3° (**NG2**) and 24.5° (**NG3**), where the pyrene cores are twisted by 12.0° and 12.9°, respectively (Figure 4d). These values are comparable to those obtained experimentally (Figure 2b). By twisting pristine pyrene, the lobes in the same phase at +*z* and –*z* sides are partly overlapped (if the *z*-axis is defined

https://doi.org/10.1021/prechem.5c00001
Precis. Chem. 2025, 3, 289–294

perpendicular to pyrene plane), which accordingly gives rise to greater effective conjugation length (Figures S59−S61). Thus, a larger twist operation leads to a narrower HOMO−LUMO gap: 3.84 eV (0°) > 3.35 eV (12.0°) > 3.26 eV (12.9°). The π-extension from the contorted pyrene core further contributes to the narrowed HOMO−LUMO gap (2.37 eV for **NG2** and 2.33 eV for **NG3**), reflecting the significant elevation of the HOMO level. Overall, the absorption/emission bands were effectively pushed to red region by both contortion of the pyrene core and the extended π-skeleton.

CONCLUSION

In summary, we achieved geometrical reinforcement of **NG2** and **NG3** as an alternatively twisted form by introducing 1,4-dioxane rings fused at the K-region of the contorted pyrene core, as is evident by smaller Stokes shifts relative to **NG1**, which fluctuates between wavy and alternatively twisted forms. It should be noted that twisting of the pyrene core with a larger degree of contortion contributes to a smaller HOMO−LUMO gap owing to unusual lobe overlapping between the $+z$ and $-z$ sides perpendicular to the pyrene plane. Even in **NG1**−NG3, the electronic character of the twisted pyrene is substantially maintained, and it becomes the cause of high quantum efficiency as well as significant bathochromic shifts of absorption/emission bands. Alongside these findings, we also elucidated cyclization induced by semi-deprotection of tetraoxa[4.4.4]propellane. As a demonstrative trial, we succeeded in obtaining a model NG (**7**) from the designed precursor **6** without the use of any oxidant. Different from conventional Scholl cyclization, where the HOMO levels of the formed NGs far higher than those of the precursors sometimes require extreme care for their isolation and/or handling, there is no concern about overoxidation of NGs obtained by the method demonstrate herein.

ASSOCIATED CONTENT

Supporting Information

The Supporting Information is available free of charge at https://pubs.acs.org/doi/10.1021/prechem.5c00001.

Detailed experimental procedures, characterization data, and computational results (PDF)

Crystal structure of **NG1′** (CIF)

Crystal structure of **NG2** (CIF)

Crystal structure of **NG3** (CIF)

Accession Codes

CCDC 2387884 (**NG1′**), 2387886 (**NG2**), and 2387885 (**NG3**) contain the supplementary crystallographic data for this paper. These data can be obtained free of charge via www.ccdc.cam.ac.uk/data_request/cif, or by emailing data_request@ccdc.cam.ac.uk, or by contacting The Cambridge Crystallographic Data Centre, 12 Union Road, Cambridge CB2 1EZ, UK; fax: + 44 1223 336033.

AUTHOR INFORMATION

Corresponding Authors

Shuqin Han − *College of Chemistry and Chemical Engineering, Inner Mongolia University, Hohhot 010021, China*; Email: chem-hshq@imu.edu.cn

Fenghua Bai − *College of Chemistry and Chemical Engineering, Inner Mongolia University, Hohhot 010021, China*; Email: f.h.bai@imu.edu.cn

Yoshifumi Hashikawa − *Institute for Chemical Research, Kyoto University, Uji, Kyoto 611-0011, Japan*; orcid.org/0000-0001-7834-9593; Email: hashi@scl.kyoto-u.ac.jp

Chaolumen − *College of Chemistry and Chemical Engineering, Inner Mongolia University, Hohhot 010021, China*; orcid.org/0009-0000-4127-6853; Email: chaolumen@imu.edu.cn

Authors

Zhenxun Xu − *College of Chemistry and Chemical Engineering, Inner Mongolia University, Hohhot 010021, China*

Suriguga Meng − *College of Chemistry and Chemical Engineering, Inner Mongolia University, Hohhot 010021, China*

Zhiyu Zhang − *College of Chemistry and Chemical Engineering, Inner Mongolia University, Hohhot 010021, China*; orcid.org/0009-0002-1574-8727

Yanping Dong − *College of Chemistry and Chemical Engineering, Inner Mongolia University, Hohhot 010021, China*

Complete contact information is available at: https://pubs.acs.org/10.1021/prechem.5c00001

Author Contributions

Z.X. and S.M. contributed equally to this work.

Notes

The authors declare no competing financial interest.

ACKNOWLEDGMENTS

Financial support was provided by the National Natural Science Foundation of China (22161035), the Education Department of Inner Mongolia Autonomous Region (NJYT22089), the Funding Scheme for High-Level Overseas Chinese Students' Return, the International Collaborative Research Program of Institute for Chemical Research (ICR), Kyoto University (2022-39 and 2023-46), JSPS KAKENHI Grant JP22H04538, Advanced Technology Institute Research Grants 2023, ISHIZUE 2024 of Kyoto University, JACI Prize for Encouraging Young Researcher, Yazaki Memorial Foundation for Science and Technology, and the Asahi Glass Foundation. We are grateful to Mr. He Meng, Mr. Yuzhan Jiao, and Prof. Jianguo Wang (Inner Mongolia University) for the support of NMR and quantum yield measurements.

REFERENCES

(1) Pascal, R. A. Twisted Acenes. *Chem. Rev.* **2006**, *106*, 4809−4819.

(2) Lu, J.; Ho, D. M.; Vogelaar, N. J.; Kraml, C. M.; Pascal, R. A., Jr. A Pentacene with a 144° Twist. *J. Am. Chem. Soc.* **2004**, *126*, 11168−11169.

(3) Duong, H. M.; Bendikov, M.; Steiger, D.; Zhang, Q.; Sonmez, G.; Yamada, J.; Wudl, F. Efficient Synthesis of a Novel, Twisted and Stable, Electroluminescent "Twistacene". *Org. Lett.* **2003**, *5*, 4433−4436.

(4) Pascal, R. A., Jr.; McMillan, W. D.; Van Engen, D. 9,18-Diphenyltetrabenz[a,c,h,j]anthracene: a remarkably twisted polycyclic aromatic hydrocarbon. *J. Am. Chem. Soc.* **1986**, *108*, 5652−5653.

(5) Xiao, J.; Duong, H. M.; Liu, Y.; Shi, W.; Ji, L.; Li, G.; Li, S.; Liu, X.-W.; Ma, J.; Wudl, F.; Zhang, Q. Synthesis and Structure Characterization of a Stable Nonatwistacene. *Angew. Chem., Int. Ed.* **2012**, *51*, 6094−6098.

(6) Norton, J. E.; Houk, K. N. Electronic Structures and Properties of Twisted Polyacenes. *J. Am. Chem. Soc.* **2005**, *127*, 4162−4163.

(7) Bedi, A.; Armon, A. M.; Diskin-Posner, Y.; Bogosalvsky, B.; Gidron, O. Controlling the helicity of π-conjugated oligomers by tuning the aromatic backbone twist. *Nat. Commun.* **2022**, *13*, 451.
(8) Bedi, A.; Shimon, L. J. W.; Gidron, O. Helically Locked Tethered Twistacenes. *J. Am. Chem. Soc.* **2018**, *140*, 8086−8090.
(9) Bedi, A.; Gidron, O. The Consequences of Twisting Nanocarbons: Lessons from Tethered Twisted Acenes. *Acc. Chem. Res.* **2019**, *52*, 2482−2490.
(10) Liu, X.; Jin, Z.; Qiu, F.; Guo, Y.; Chen, Y.; Sun, Z.; Zhang, L. Hexabenzoheptacene: A Longitudinally Multihelicene Nanocarbon with Local Aromaticity and Enhanced Stability. *Angew. Chem., Int. Ed.* **2024**, *63*, No. e202407547.
(11) Yang, W.-W.; Ren, Z.-H.; Feng, J.; Lv, Z.-B.; Cheng, X.; Zhang, J.; Du, D.; Chi, C.; Shen, J.-J. A Deep-Red Emissive Sulfur-Doped Double [7]Helicene Photosensitizer: Synthesis, Structure and Chiral Optical Properties. *Angew. Chem., Int. Ed.* **2024**, *63*, No. e202412681.
(12) Wu, Y. F.; Zhang, L.; Zhang, Q.; Xie, S. Y.; Zheng, L. S. Multiple [*n*]Helicenes with Various Aromatic Cores. *Org. Chem. Front.* **2022**, *9*, 4726−4743.
(13) Arrico, L.; Di Bari, L. D.; Zinna, F. Quantifying the Overall Efficiency of Circularly Polarized Emitters. *Chem. - Eur. J.* **2021**, *27*, 2920−2934.
(14) Bernhardt, A.; Cavlovic, D.; Mayländer, M.; Blacque, O.; Cruz, C. M.; Richert, S.; Juríček, M. π-Radical Cascade to a Chiral Saddle-Shaped Peropyrene. *Angew. Chem., Int. Ed.* **2024**, *63*, No. e202318254.
(15) Penty, S. E.; Orton, G. R. F.; Black, D. J.; Pal, R.; Zwijnenburg, M. A.; Barendt, T. A. A Chirally Locked Bis-perylene Diimide Macrocycle: Consequences for Chiral Self-Assembly and Circularly Polarized Luminescence. *J. Am. Chem. Soc.* **2024**, *146*, 5470−5479.
(16) Eichelmann, R.; Jeudy, P.; Schneider, L.; Zerhoch, J.; Mayer, P. R.; Ballmann, J.; Deschler, F.; Gade, L. H. Chiral *Bay*-Alkynylated Tetraazaperylenes: Photophysics and Chiroptical Properties. *Org. Lett.* **2024**, *26*, 1172−1177.
(17) Bam, R.; Yang, W.; Longhi, G.; Abbate, S.; Lucotti, A.; Tommasini, M.; Franzini, R.; Villani, C.; Catalano, V. J.; Olmstead, M. M.; Chalifoux, W. A. Chiral Teropyrenes: Synthesis, Structure, and Spectroscopic Studies. *Angew. Chem., Int. Ed.* **2024**, *63*, No. e202404849.
(18) Liu, Y.; Li, Z.; Wang, M.-W.; Chan, J.; Liu, G.; Wang, Z.; Jiang, W. Highly Luminescent Chiral Double π-Helical Nanoribbons. *J. Am. Chem. Soc.* **2024**, *146*, 5295−5304.
(19) Dubey, R. K.; Melle-Franco, M.; Mateo-Alonso, A. Inducing Single-Handed Helicity in a Twisted Molecular Nanoribbon. *J. Am. Chem. Soc.* **2022**, *144*, 2765−2774.
(20) Swain, A.; Radacki, K.; Braunschweig, H.; Ravat, P. Helically twisted nanoribbons via stereospecific annulative π-extension reaction employing [7]helicene as a molecular wrench. *Chem. Sci.* **2024**, *15*, 11737−11747.
(21) Li, Y.; Jia, Z.; Xiao, S.; Liu, H.; Li, Y. A method for controlling the synthesis of stable twisted two-dimensional conjugated molecules. *Nat. Commun.* **2016**, *7*, 11637.
(22) Castro-Fernández, S.; Cruz, C. M.; Mariz, I. F. A.; Márquez, I. R.; Jiménez, V. G.; Palomino-Ruiz, L.; Cuerva, J. M.; Maçôas, E.; Campaña, A. G. Two-Photon Absorption Enhancement by the Inclusion of a Tropone Ring in Distorted Nanographene Ribbons. *Angew. Chem., Int. Ed.* **2020**, *59*, 7139−7145.
(23) Izquierdo-Garcia, P.; Fernández-García, J. M.; Fernandez, I.; Perles, J.; Martín, N. Helically Arranged Chiral Molecular Nanographenes. *J. Am. Chem. Soc.* **2021**, *143*, 11864−11870.
(24) Cheung, K. Y.; Chan, C. K.; Liu, Z.; Miao, Q. A Twisted Nanographene Consisting of 96 Carbon Atoms. *Angew. Chem., Int. Ed.* **2017**, *56*, 9003−9007.
(25) Oki, K.; Takase, M.; Mori, S.; Shiotari, A.; Sugimoto, Y.; Ohara, K.; Okujima, T.; Uno, H. Synthesis, Structures, and Properties of Core-Expanded Azacoronene Analogue: A Twisted π-System with Two N-Doped Heptagons. *J. Am. Chem. Soc.* **2018**, *140*, 10430−10434.
(26) Suleymanov, A. A.; He, Q.; Müller, P.; Swager, T. M. Highly Contorted Rigid Nitrogen-Rich Nanographene with Four Heptagons. *Org. Lett.* **2024**, *26*, 5227−5231.
(27) Liu, J.; Hong, J.; Liao, Z.; Tan, J.; Liu, H.; Dmitrieva, E.; Zhou, L.; Ren, J.; Cao, X.-Y.; Popov, A. A.; Zou, Y.; Narita, A.; Hu, Y. Negatively Curved Octagon-Incorporated Aza-nanographene and its Assembly with Fullerenes. *Angew. Chem., Int. Ed.* **2024**, *63*, No. e202400172.
(28) Dong, Y.; Zhang, Z.; Hashikawa, Y.; Meng, H.; Bai, F.; Itami, K.; Chaolumen. A Double Twisted Nanographene with a Contorted Pyrene Core. *Angew. Chem., Int. Ed.* **2024**, *136*, No. e202406927.
(29) Wallerius, C.; Erdene-Ochir, O.; Doeselar, E. V.; Alle, R.; Nguyen, A. T.; Schumacher, M. F.; Lützen, A.; Meerholz, K.; Pun, S. H. Quadruple[6]Helicene Featuring Pyrene Core: Unraveling Contorted Aromatic Core with Larger Effective Conjugation. *Precis. Chem.* **2024**, *2*, 488−494.
(30) Hummelen, J. C.; Knight, B.; Pavlovich, J.; González, R.; Wudl, F. Isolation of the Heterofullerene $C_{59}N$ as Its Dimer $(C_{59}N)_2$. *Science* **1995**, *269*, 1554−1556.
(31) Keshavarz-K, M.; González, R.; Hicks, R. G.; Srdanov, G.; Srdanov, V. I.; Collins, T. G.; Hummelen, J. C.; Bellavia-Lund, C.; Pavlovich, J.; Wudl, F.; Holczer, K. Synthesis of hydroazafullerene $C_{59}HN$, the parent hydroheterofullerene. *Nature* **1996**, *383*, 147−150.
(32) Hashikawa, Y.; Murata, M.; Wakamiya, A.; Murata, Y. Synthesis and Properties of Endohedral Aza[60]fullerenes: $H_2O@C_{59}N$ and $H_2@C_{59}N$ as Their Dimers and Monomers. *J. Am. Chem. Soc.* **2016**, *138*, 4096−4104.
(33) Hashikawa, Y.; Murata, Y. Facile Access to Azafullerenyl Cation $C_{59}N^+$ and Specific Interaction with Entrapped Molecules. *J. Am. Chem. Soc.* **2017**, *139*, 18468−18471.

https://doi.org/10.1021/prechem.5c00001
Precis. Chem. 2025, 3, 289−294